Bubble cavitation generation near the blood vessel wall by amplitude-modulated wave irradiation

Ren Koda[1†], Taichi Mukai[1] , and Yoshiki Yamakoshi([1]Grad. School Sci. and Tech., Gunma Univ.)

1. Introduction

In vivo bubble cavitation applications such as sonoporation and drug delivery are promising methods to increase drug permeablity. Micro hollows are produced by microjets caused by microbubble cavitation. However, sonoporation consists of several mechanisms that are triggered simultaneously [1]. Due to the secondary Bjerknes force acting between adjacent bubbles, the microbubbles aggregate to form a bubble cloud. Bubble clouds exhibit complex movements in the ultrasound acoustic field due to the primary Bjerknes force. The non-linear oscillation of the bubbles causes the bubble cloud to burst. We have proposed an image reconstruction technique that enables both temporal- and spatial-resolved observation of bubble cavitation dynamics using the back propagation of acoustic cavitation emission (ACE) signals [2]. Several methods have been reported as microbubble manipulation techniques, for example, utilizing the secondary Bjerknes force generated between the actual bubble and the mirror bubble to promote the adhesion of the bubble to the blood vessel wall [3].

Ideally, generating bubble destruction near the blood vessel wall would be a useful mechanism in sonoporation as it increases the biological effect near the target. In this study, we investigate an efficient irradiation sequence using amplitude-modulated waves to cause bubble destruction near the blood vessel wall and suppress bubble destruction at the center of the blood vessel far from the wall.

2. Experimental set up

Fig.1(a) and (b) show the experimental setup for ACE signal acquisition and optical observation. In Fig.1(a), we prepared a block of agarose gel as a phantom in which a rectangular-shaped hole (cross section: 2.0 mm × 5.0 mm) was made in order to inject a bubble suspension. In Fig.1(b), we prepared a block of agarose gel as a phantom in which a rectangular-shaped hole (cross section: 2.0 mm × 2.0 mm) was made in order to inject a bubble suspension. A concave transducer was adopted for pumping US irradiation. The center frequency of pumping US was 2.5 MHz. The focal length of the pumping US transducer was 42 mm and the beam

koda@gunma-u.ac.jp
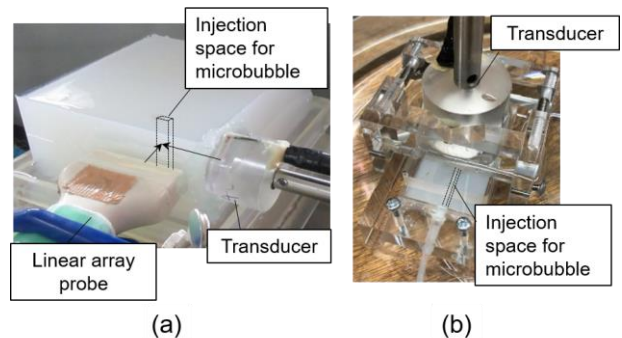
Fig. 1 Experimental set up for ACE signal acquisition (a), and for optical observation (b)

width of pumping US at the focal point was about 2 mm.

We used microbbules of Sonazoid (Daiichi Sankyo, Japan), which have a phospholipid shell and perfluorobutane inside with an average diameter of between 2 and 3 μm. The suspension of microbubbles was prepared just before the experiment at a concentration of 1.2×10^6 bubbles / mL, which was diluted 1000 times from the original preparation of Sonazoid.

To record the RF signals, an ultrasound platform (RSYS0003, Microsonic Co. Ltd., Japan) with an imaging linear array probe was chosen. The array has 64 elements with a 7.5 MHz central frequency, a 38.4-mm aperture, and a 0.6 mm element pitch width. In beamforming the received signals, 16 channel data were simultaneously captured, and the frame reconstruction is performed using 32 beamlines. Individual beamlines are formed at intervals with a duration equal to the pulse-repetition time (80 μs). The reconstructed image is obtained at the rate of 390.6 Hz with the irradiation of the pumping US pulse.

We consider the sound input to be a combination of carrier signal (sine wave) of frequency f_c and modulating signal (sine wave) of a frequency f_m having the same amplitude. The amplitude-modulated wave is

$$s_m(t) = \{1 + cos(2\pi f_m t) \} \times cos(2\pi f_c t) \quad (1)$$

If the envelope length of the amplitude-modulated wave is λ_c, the relationship between f_m and λ_c is

$$\frac{1}{4}\lambda_c = \frac{v}{2f_m} \qquad (2)$$

3. Results

To eliminate the non-linear oscillation component, we applied a digital filter combined with a band stop filter designed to cut the higher harmonic components within the frequency band range of the linear array probe. Fig. 2 shows the reconstructed amplitude signal image which acquired under pumping US exposure with amplitude-modulated signal. The sound pressure is modulated to repeat up to 1.4 MPa over a duration of 40 μs. In Fig. 2, the cavitation distribution appears alternately in the vicinity of w_1 and w_2 in synchronization with the modulated period of the amplitude-modulated wave.

In order to examine the difference in cavitation generation efficiency depending on the waveform of the pumping US wave, we compared a sine wave and an amplitude-modulated wave whose sound pressure was adjusted so that the acoustic energy was uniform. Fig. 3 shows a comparison of total signal amplitude for 20 frames of sine wave and amplitude-modulated wave irradiation. The total signal amplitude during amplitude-modulated wave irradiation was larger than that during sine wave irradiation at ROI A, B, and C.

Figure 4 shows examples of optical observation of the wall surface of a blood vessel phantom trimmed in the ROI range irradiated with
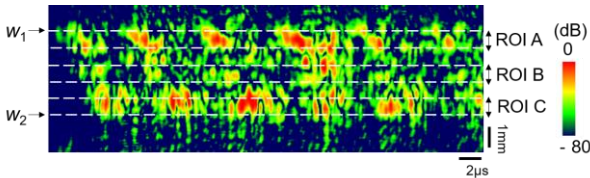
Fig. 2 Typical example of ACE image during AM wave irradiation.
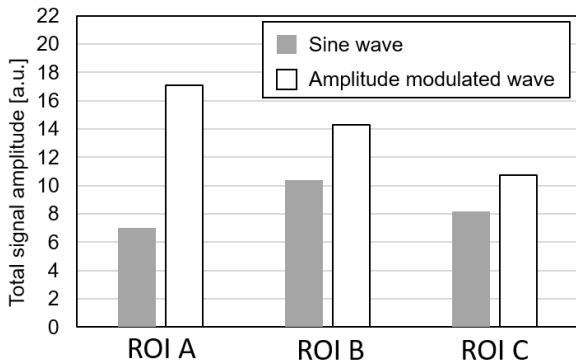
Fig. 3 Comparison of total signal amplitude for 20 frames of sine wave and amplitude-modulated wave irradiation.
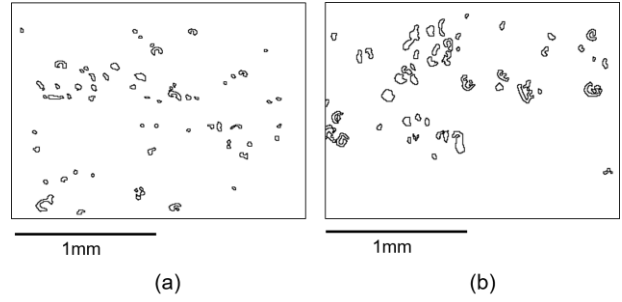
Fig. 4 Examples of binary optical observation of blood vessel phantom wall surface
(a) Sine wave irradiation (b) Amplitude modulated wave irradiation.
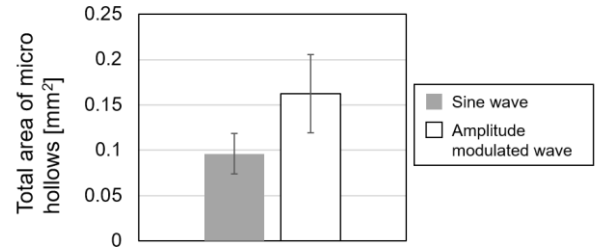
Fig. 5 Area comparison of micro hollows on the wall surface of blood vessel phantom.

the sine and the amplitude-modulated waves. The ROI size is set to 1.6 [mm] x 2 [mm].

Figure 5 shows an area comparison of micro hollows on the wall surface of blood vessel phantom. The mean values and the standard deviations of the seven trials are shown. The area of the micro hollows irradiated with the amplitude modulated wave was 1.9 times that of the sine wave.

4. Conclusion

We proposed an efficient irradiation sequence using amplitude-modulated waves for efficient cavitation generation. As a result, it was suggested that the acoustic perforation effect of the proposed sequence was more efficient than the energy-aligned sine wave irradiation sequence.

References
1. Y. Yamakoshi, J. Yamaguchi, T. Ozawa, T. Isono, and T. Kanai, Jpn. J. Appl. Phys. **52** (2013) 07HF12.
2. R. Koda, T. Origasa, T. Nakajima and Y. Yamakoshi, IEEE Trans Ultrason Ferroelectr Freq Control, **66** (2019) 823.
3. Yamakoshi and T. Miwa, Jpn. J. Appl. Phys. **50** (2011) 07HF01.